Am J Transl Res 2020;12(9):5399-5415
www.ajtr.org /ISSN:1943-8141/AJTR0112246

*Original Article*

# The combination of circRNA-UMAD1 and Galectin-3 in peripheral circulation is a co-biomarker for predicting lymph node metastasis of thyroid carcinoma

Wenbin Yu[1*], Bo Ma[2*], Wei Zhao[3], Jingtao Liu[4], Hao Yu[1], Zhihua Tian[5], Zhiqin Fan[6], Haibo Han[7]

*Departments of [1]Hand and Neck Surgery, [2]Lymphoma, [3]Cell Biology, [4]Pharmacy, [5]Central Laboratory, Key Laboratory of Carcinogenesis and Translational Research (Ministry of Education), Peking University Cancer Hospital and Institute, Beijing 100142, P. R. China; [6]Day Surgery Department, Affiliated Tumor Hospital of Xinjiang Medical University, Urumqi 830011, P. R. China; [7]Department of Clinical Laboratory, Key Laboratory of Carcinogenesis and Translational Research (Ministry of Education), Peking University Cancer Hospital and Institute, Beijing 100142, P. R. China. [*]Equal contributors.*

Received April 10, 2020; Accepted August 7, 2020; Epub September 15, 2020; Published September 30, 2020

**Abstract:** The diagnosis of lymph node metastasis (LNM) by liquid biopsy is a novel concept prompted by the necessity to develop a more convenient and accurate method to guide the clinical management of early LNM in papillary thyroid carcinoma (PTC). However, the sensitivity and specificity of many biomarkers are not high enough. We aimed to detect circRNAs from peripheral circulation that may be better associated with the prognosis of LNM in PTC. First, Galectin-3 (Gal3) in blood was determined to be highly expressed in LNM patients. Second, based on a bioinformatics analysis and miRNA sequencing analysis from 2 paired primary and LNM tumors, miR-873 was identified to directly target Gal3, which was significantly associated with clinical parameters including LNM. Third, from additional circRNA sequencing, circRNA-UMAD1 was selected as a specific sponge for miR-873 and was correlated with Gal3 levels in peripheral circulation. Fourth, circRNA-UMAD1 and Gal3 were identified to have stronger co-biomarker potential with relatively high expression in the serum of LNM patients compared with primary tumor patients, as demonstrated by the RNA expression levels in the serum of 50 PTC patients with or without LNM by quantitative real-time PCR. Overall, the combination of circRNA-UMAD1 and Gal3 is a useful and effective co-biomarker for the prognosis of LNM in PTC patients. This new molecular typing method for LNM in PTC is more precise.

**Keywords:** CircRNA UMAD1, Gal3, miRNA-873, papillary thyroid carcinoma, lymph-node metastasis

## Introduction

The risk factors for rapid growth and early metastasis of papillary thyroid carcinoma (PTC) have been assessed to strongly predict the patient advantage of thyroidectomy with or without lymphadenectomy in the last decade [1, 2]. However, the value of molecular analyses of PTC tissues and laboratory blood tests is not yet fully appreciated. The safety and efficiency of liquid biopsy have been demonstrated in recent years [3] with the development of molecular diagnostic techniques in many solid tumors [4], such as lung cancer and liver cancer, that have low detection rate due to lack of adequate tumor tissues, pathological histological limitations, and long monitoring periods. However, this technology is seldom used in thyroid carcinoma and has been limited to miRNAs, BRAF and P53 mutations [5-7].

Liquid biopsy is a novel method for finding new strategies to better understand the progression of thyroid carcinoma [8] and may predict features of lymph node metastasis (LNM) in advanced PTC patients, such as serum P53 protein expression [9]. New driver genes and the presence of mutations in tumors were found easily [10, 11]. Therefore, a sensitive, convenient and efficient prediction system from peripheral circulation would be viable and valuable for LNM in PTC.

Circular RNAs (circRNAs) are widely involved in human tumor tissues and developmental and disease processes [12]. CircRNAs are also involved in gene regulation in PTC [13]. As a newly identified class of noncoding RNA molecules, circRNAs can function in various ways, such as sponge miRNAs to release the inhibitory effect of miRNA targets [14], translate specific pep-

tides [15] or interact with RNA binding protein for protein regulation [16]. In 2018, the differential landscape of circular RNA profiles in PTC between tumor and adjust tissues was reported by Lan, X and colleagues [17]. Based on circRNA sequencing, potential tumor biomarkers were found, but not ones relevant to lymph node metastasis in PTC. Hence, in this study, we screened the sequencing data of primary tumor and lymph node metastasis and identified circ-UMAD1 as a possible circRNA that was associated with the N stage and functioned as a sponge for miRNA-873. As a direct target of miR-873, Gal3, a member of the beta-galactoside-binding protein family, was upregulated in lymph node metastatic samples, which was validated in peripheral circulation. Gal3 functions as a modulator of cell growth through its galactoside-binding function and is correlated with the occurrence and metastasis of papillary thyroid carcinoma [18, 19]. In our previous study, we found that secreted Gal3 was strongly associated with tumor malignant behaviors and the migration of tumor cells [20]. Chen C and colleagues reported that circulating Gal3 induced the secretion of metastasis-promoting cytokines to participate in tumor genesis [21]. Therefore, we are interested in secreted Gal3 in serum to avoid unnecessary aggressive interventions and propose to use it as a potential marker for diagnosing LNM in PTC, as Yilmaz E reported [22]. However, only detecting Gal3 does not have sufficient diagnostic value for PTC. We demonstrate that combining circRNA-UMAD1 and Gal3 expression analysis is a more useful and accurate co-biomarker for the prediction of LNM in patients with PTC and warrants further studies of the potential roles of this co-biomarker in PTC lymph node metastasis.

## Material and methods

### *Patients*

Fifty papillary thyroid carcinoma (PTC) patients who underwent thyroidectomy with or without lymphadenectomy at the Peking University Cancer Hospital (PUCH) were included in this study. All of these patients had local primary and metastatic PTC, which was diagnosed by histological or cytological validation. All patients had a complete electronic medical case history without an identified target lesion. Random tissues from paired primary tumors and lymph nodes were sequenced by Micrqread Biotech Company, China using circRNA and miRNA next generation sequencing technology. The entire samples were immediately snap frozen in liquid nitrogen and stored at -196°C after resection for subsequent experiments. The acquisition and use of these tissues were performed with informed consent according to a protocol approved by the Ethics Committee of PUCH.

### *Plasma sample preparation*

Fresh peripheral blood samples were obtained before surgery. Plasma samples were collected within 2 hours in EDTA tubes and were isolated by spin down. One aliquot of plasma samples was immediately used for RNA extraction without frozen, and the other aliquots were transported frozen to storage at -80.

### *miRNA extraction and circRNA enrichment*

Total RNA, which included miRNA, was extracted using the Qiagen miRNeasy Mini Kit (Qiagen, Hilden, Germany) from 300 ml fresh plasma following the manufacturer's protocol. To enrich cfRNA, the samples were incubated with 5 U RNase R for 30 minutes at 37°C in a 20 ml reaction. Then, they were purified using a Qiagen RNeasy MiniElute Purification Kit (Qiagen, Hilden, Germany) according the manufacturer as previously reported [23].

### *Reverse transcription and quantitative real-time PCR*

First strand cDNA was synthesized from 10 ng RNA with an M-MLV transcription Kit (Qiagen) with random primers according the manufacturer's instructions. Quantitative PCR was performed with PowerUp™ SYBR Green Mater Mix (Applied Biosystems Thermo Fisher Scientific). The forward and reverse sequences of circRNA-UMAD1 primers and miR-873 were designed by RiboBio Biotechnology Company. Each sample was analyzed in triplicate on the ABI Prism 7500 Fast (Applied Biosystems) according to the manufacturer's instructions as previously reported. Data are presented as relative quantification (RQ) to U6 or GAPDH, based on $2^{-\Delta Ct}$ values where ΔCt = Ct (Target) - Ct (Reference). Fold change was calculated by the $2^{-\Delta Ct}$ method.

### *Bioinformatic data mining*

We downloaded TCGA TC RNA-Seq gene expression data, miRNA data and clinical data

from the LinkedOmics website [24]. Predictions of potential targets of miR-873 were performed by computational algorithms based on 'seed regions' between miRNAs and target genes. miRanda (http://miRdb.org/miRDB/index.html), TargetScan (http://www.targetscan.org), and miRGen v.3 (http://carolina.imis.athena-innovation.gr/diana_tools/web/index.php?r=miRgenv3%2Findex) were used in this study [25-27]. We screened the miRNAs that were significantly negatively correlated with overall survival and N stage of patients with PTC in The Cancer Genome Atlas (TCGA) dataset. Predicting circRNAs that acted as sponges of miRNAs was performed by website tools (Circular RNA Interactome from NIH) [28]. All tumors had corresponding clinical data that were used to perform the clinical correlation and survival analysis. Fifty-five normal and 505 TC tissues had detectable Gal3 mRNA expression. In total, 152 non-LNM PTC tissues and 109 LNM PTC tissues had detectable hsa-mir-873 expression. All 261 TC tumors with or without LNM had clinical data that was used for clinical correlation analysis.

*Western blot analysis*

Protein of tissues were extracted in an appropriate volume of lysis buffer (50 mM Tris pH 7.4, 150 mM NaCl, 1% NP-40, 0.25% sodium deoxycholate. 0.1% SDS) supplemented with 1 mM PMSF, phosphatase inhibitor cocktail, and Complete Mini Protease Inhibitor Cocktail (Roche, Mannheim, Germany). Normal lymph nodes and tumor metastasis lymph nodes from patients No. 325, 353, 323 and 759 were resolved and electroblotted onto nitrocellulose membranes by 10% SDS-PAGE according to standard protocols. The membranes were incubated with primary antibodies specific to Gal3 (Cell Signaling, #87985), NOTCH1 (Cell Signaling, #3608), Hes1 (Cell Signaling, #11-988), TGF-β1 (Abcam, ab92486), ErbB2 (Abcam, ab237715), ErbB4 (Abcam, ab19391), NF-κB (p65) (Abcam, ab7970) and GAPDH (Bioworld BS606030), also corresponding secondary HRP-conjugated goat anti-rabbit (Jackson.US) were immunoreacted. The bands were visualized by Immobilon™ Western Kit (Millipore, Billerica, MA) using a MiniChemi imaging system (Sagecreation, China).

*Indirect dual immunofluorescence*

Indirect dual immunofluorescent staining for expression of Gal3 and ErbB4 in tumor and LNM slides was performed as described previously [20].

*Secreted Gal3 expression in blood by ELISA analysis*

Gal3 activity in the peripheral blood from TC cells was measured with an Amplite Fluorimetric Assay Kit (AAT Bioquest Inc., CA, USA) following the protocols provided by the manufacturer as described [20].

*Luciferase reporter assay*

The 3'-UTRs of Gal3 carrying the putative miR-873 binding sites and the mutant binding sites were amplified by PCR and were inserted immediately downstream of the firefly luciferase cDNA in the pGL3-control vector (Promega, Madison, WI, USA) to construct pGL3-Gal3 WT and pGL3-Gal3 MUT. For the luciferase assay, $10^5$ cells per well were cultured in 24-well plates. Using Lipofectamine 2000, the pGL3 constructs and the pRL-TK plasmid, (Renilla luciferase) were cotransfected with miR-873 or miR-873 control (Invitrogen). The activities of firefly luciferase and Renilla luciferase were measured at 24 h posttransfection using a Dual-Luciferase Reporter Assay Kit (Promega) according to the manufacturer's protocol. Firefly luciferase activity was normalized to that of Renilla luciferase for each sample. Each experimental group consisted of four wells, and the experiment was repeated three times.

*Statistical analysis*

All experiments were performed independently in triplicate. The unpaired two-sided Student's t-test for independent samples with Excel 2010 software was used to compare the difference in circRNAs between two groups, and data are presented as the median ± range. In the case of multiple comparisons, one-way ANOVA followed by Bonferroni-Holm procedure was applied. Correlation was performed using two-tailed Spearman's test. $P<0.05$ was considered significant.

## Results

*Gal3 in peripheral circulation is associated with lymph node metastasis in PTC patients*

Gal3 has been shown to serve as a potential marker for LNM in PTC by analyzing a total of 424 patients across six eligible studies [18], and it is highly expressed in thyroid cancer

compared to many other solid cancers by analysis of data from *The Human Protein Atlas*, which is a Swedish-based program aiming to map all human proteins in cells and tissues of 17 main cancer types using data from 8000 patients (**Figure 1A**). Based on these observations, we decided to validate Gal3 expression in peripheral circulation between patients who were diagnosed with PTC with or without LNM at PUCH. 12 men and 48 women aged from 24-63 were recognized PTC with one thyroid side (44 cases) or both thyroid sides (6 cases) underwent thyroidectomy with (27 cases) or without lymphadenectomy (23 cases). As shown in **Table 1** and **Figure 1B**, the levels of Gal3 were highly significant in the blood of LNM patients compared with no metastasis patients. Gal3 levels were associated with clinical LNM properties significant in the PUCH samples (**Figure 1C**). Analysis of TCGA e data on PTC showed that Gal3 was not only highly expressed in PTC tumors compared with normal tissues (**Figure 1D**) but was strongly correlated to stage and LNM (**Figure 1E**, **1F**). These data suggest that Gal3 is a useful biological tool for diagnosing LNM in PTC. However, it was not the best one among all the positively correlated significant genes associated with LNM (**Figure 1G**).

*Enrichment of circRNAs and miRNAs in LNM tissues*

Because only detecting Gal3 had limitations in predicting LNM, we propose that other elements are more sensitive biomarkers for LNM. To determine the value of circulating circRNAs and miRNAs, sequencing was performed to identify which circRNAs and miRNAs were upregulated in LNM samples (**Figure 2A**), which were verified to have LNM properties by pathological diagnosis (**Figure 2B**). The normalized intensities of the detected ceRNAs were similar across all samples, and the heat map shows that the different circRNAs and miRNAs were divided into distinct groups of PTC primary tumors and LNM tumors (**Figure 2C**, **2D**). A total of 208 circRNAs and 134 miRNAs were upregulated and 184 circRNAs and 86 miRNAs were downregulated in the LNM group. KEGG pathway analysis revealed many biological processes involved in cancer and lymphoid tissues for circRNAs and miRNAs, respectively (**Figure 2E**, **2F**). ErbB, NOTCH, NF-κB and TGF-β pathways were analyzed by Western blot between normal and metastasis of lymph node form PTC patients (**Figure 2G**), and IF were performed that Galectin3 and ErbB4 protein levels were strongly expressed in LNM of PTC (**Figure 2H**). These results indicated that ceRNAs in circulation could be used as biomarkers to predict LNM potential and the clustering ceRNAs from LNM implicated that involvement of ErbB and NF-κB pathways were reasonable to LNM.

*miR-873 is associated with Gal3*

miRNAs are useful diagnostic indicators [29]. Using TCGA profiling data (**Figure 3A**), we found that miR-873 was one of the top genes associated with LNM in PTC patients, and miR-873 was predicted to target Gal3 by screening miRNA sequencing data and prediction analyses by 3 miRNA databases (**Figure 3B**). Next, we performed a luciferase reporter assay with a vector containing the 3'-UTR of Gal3 that flanked the putative binding sites of miR-873 in Gal3. Mutations were generated in the putative binding sites, which were used as controls (**Figure 3C**). As shown in **Figure 3D**, a statistically significant inhibition of luciferase activity was observed in the wild-type Gal3 3'-UTR compared with the mutant construct or with the cotransfection of pcDNA3.0. The inhibition rate for the wild-type 3'-UTR of Gal3 was 57% compared with the corresponding rate of the mutant 3'-UTR. Hence, the miR-873 binding sites in the 3'-UTR of Gal3 were responsible for the inhibition of reporter activity, which suggests that miR-873 directly modulates the expression of this gene through its 3'-UTR. Moreover, qRT-PCR analysis confirmed the expression of Gal3 in 293FT cells that were transfected with miR-873 mimic or inhibitor (**Figure 3E**, **3F**). Furthermore, the circulating miR-873 was validated by qRT-PCR in all serum samples. Consistent with the TCGA data (**Figure 3G**, **3H**), the level of miR-873 was stronger in LNM patients than in primary PTC patients (**Figure 3I**). Thus, miR-873 is a candidate for direct targeting of Gal3 and contributes LNM in PTC.

*Circulating circRNA-UMAD1 acts as a miR-873 sponge*

Based on the exploration of the differential miR-873 expression in the circulation of PTC patients with or without LNM, differentially expressed circRNAs were screened with the criteria of fold change >2, $P$ value <0.05 and association with miR-873 by website prediction tools (**Figure 4A**, upper). Increasing evi-

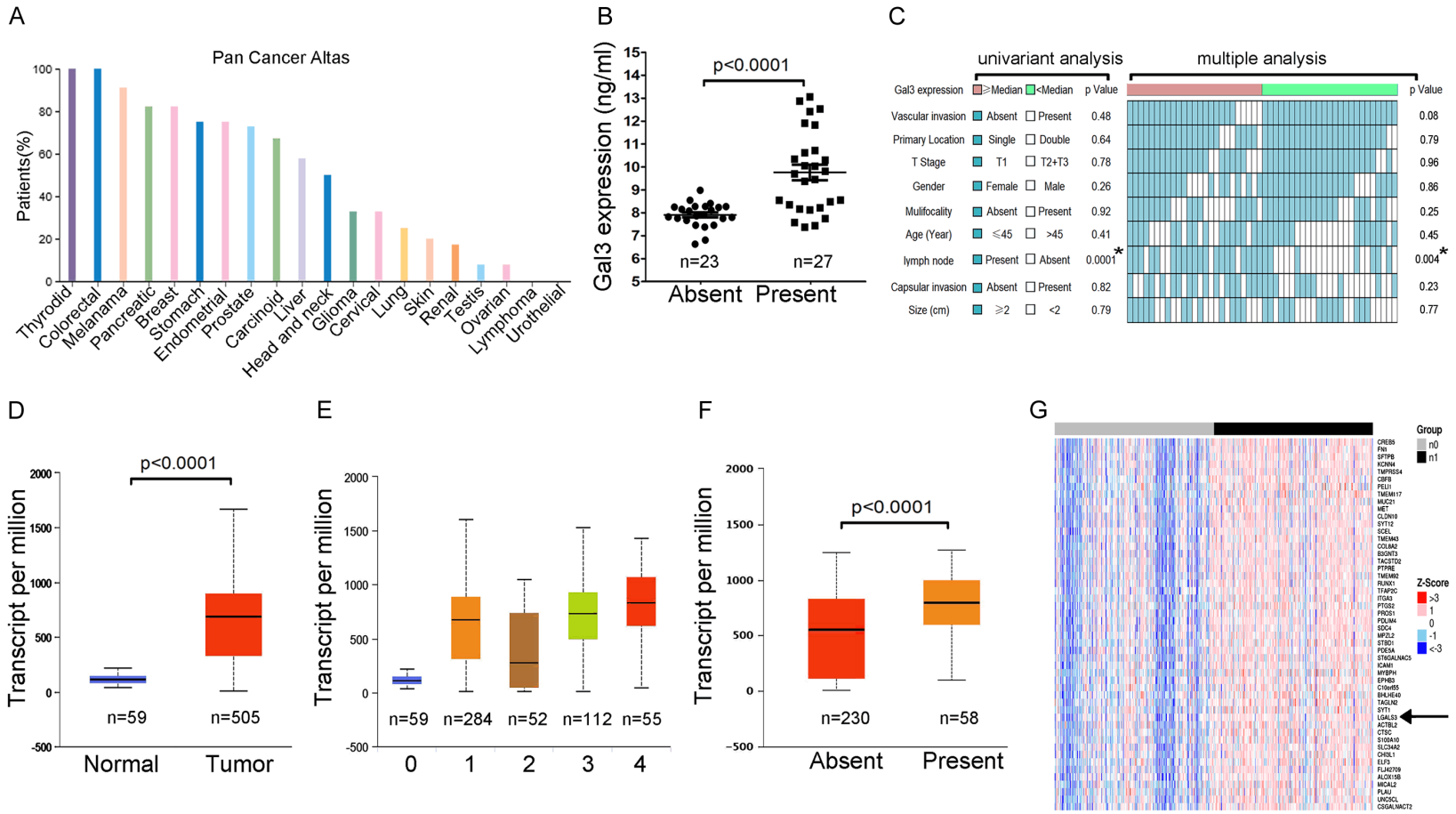


**Figure 1.** Circulating Gal3 is a potential target for the diagnosis of LNM. TCGA database analysis of the expression level of Gal3 in serval solid cancer indicated that Gal3 is 100% positive in thyroid cancer, which is more than the rate in other cancers (A). The protein level of Gal3 in the serum of PTC patients was detected by ELISA analysis, showing that LNM patients express more Gal3 (B). Gal3 expression is significantly related to LNM based on univariant analysis in 50 PTC patients (C). Sequencing TCGA data downloaded from the LinkedOmics website demonstrated that the RNA level of Gal3 is upregulated in tumor tissues (D), and is associated with the stage of PTC (E) and LNM (F). Unsupervised hierarchical clustering heat map shows the expression of different genes between non-LNM and LNM PTC samples (G). Unpaired t-test and One-way ANOVA multiple comparisons test were performed to obtain *P* values in comparisons of two or more groups. * indicates P<0.05.

**Table 1.** Relationship between Gal3 expression and pathological features in PTC patients with or without LNM

| Variable | Case no. | Gal3 expression[1] (RQ: $2^{-\Delta Ct}$) | | $P^2$ | Gal3 expression[1] (ΔCt) | $P^3$ |
|---|---|---|---|---|---|---|
| | | Median | Range | | Mean ± SEM | |
| Gender | | | | 0.2577 | | 0.8048 |
| Male | 12 | 8.994 | 7.561-11.91 | | 9.368±0.4401 | |
| Female | 38 | 8.231 | 6.614-13.06 | | 8.751±0.2689 | |
| Age | | | | 0.4056 | | 0.8592 |
| ≤45 | 29 | 8.467 | 7.357-12.88 | | 9.064±0.3095 | |
| >45 | 21 | 8.226 | 6.614-13.06 | | 8.672±0.3487 | |
| Size | | | | 0.7896 | | 0.7745 |
| <2 | 24 | 8.143 | 7.364-12.88 | | 8.723±0.3091 | |
| ≥2 | 26 | 8.335 | 6.614-13.06 | | 8.840±0.3101 | |
| Side location | | | | 0.6465 | | 0.2355 |
| Single (Left or Right) | 44 | 8.247 | 6.614-13.06 | | 8.859±0.2571 | |
| Double | 6 | 9.525 | 7.747-10.34 | | 9.190±0.4093 | |
| Capsular invasion | | | | 0.8150 | | 0.2407 |
| Absent | 26 | 8.326 | 6.614-13.06 | | 8.952±0.3584 | |
| Present | 24 | 8.250 | 6.792-12.42 | | 8.842±0.2919 | |
| Vascular invasion | | | | 0.4873 | | 0.1090 |
| Absent | 45 | 8.226 | 6.614-13.06 | | 8.776±0.2449 | |
| Present | 5 | 9.686 | 8.976-11.91 | | 10.01±0.5044 | |
| Lymph node metastasis | | | | <0.0001* | | <0.0001* |
| Absent | 23 | 7.898 | 6.614-8.976 | | 7.895±0.1112 | |
| Present | 27 | 9.686 | 7.537-13.06 | | 9.754±0.3408 | |
| T stage | | | | 0.7788 | | 0.7803 |
| T1 | 42 | 8.247 | 6.614-13.06 | | 8.870±0.2586 | |
| T2+T3 | 8 | 8.854 | 7.653-11.83 | | 9.050±0.5225 | |
| Multifocality | | | | 0.9211 | | 0.4667 |
| Absent | 34 | 8.231 | 6.792-13.06 | | 8.782±0.2844 | |
| Present | 16 | 8.948 | 6.614-12.42 | | 9.147±0.4005 | |

[1]Quantified by qRT-PCR. Gal3 was normalized to GAPDH. [2]Mann-Whitney U test for the comparison between two groups or Kruskal-Walis test for more groups. [3]Unpaired Student's t-test for the comparison between two groups. *$P$<0.05.

dence has indicated that circRNAs cloud act as a sponge for miRNAs to limit miRNA function in PTC [30], and our bioinformatics analysis identified 3 circRNAs hsa_circ_0000111, hsa_circ_0000277, and hsa_circ_0001676 that were predicted to have putative binding sites with a complementary region of miR-873 (**Figure 4A**, bottom). Using an HPA RNA-seq normal tissues analysis (BioProject PRJEB43-37) [31], two of the parent genes encoding the circRNAs, hsa_circ_0000111 and hsa_circ_0000277, were not considered for use as targets because of the high background levels in lymph nodes (**Figure 4B**). Ultimately, hsa_circ_0001676 was verified as a candidate for consideration. Furthermore, complementary binding was confirmed by dual-luciferase reporter assay (**Figure 4C**, **4D**). The negative correlation between hsa_circ_0001676 and miR-873 expression in PTC samples was identified by Pearson's correlation analysis (**Figure 4E**). Thus, the above results indicate that hsa_circ_0001676 directly targets miR-873 and acts as a sponge to miR-873.

*Circulating circRNA-UMAD1 has potential prognostic value for diagnosis of LNM*

To identify circRNA-miRNA associations is beneficial for the diagnosis of LNM, and hsa_circ_0001676 met screening criteria. The parent gene of this circRNA encodes the protein UMAD1, which was associated with lymph node expression in our PTC samples (**Figure 5A**). Consistent with the sequencing results, the

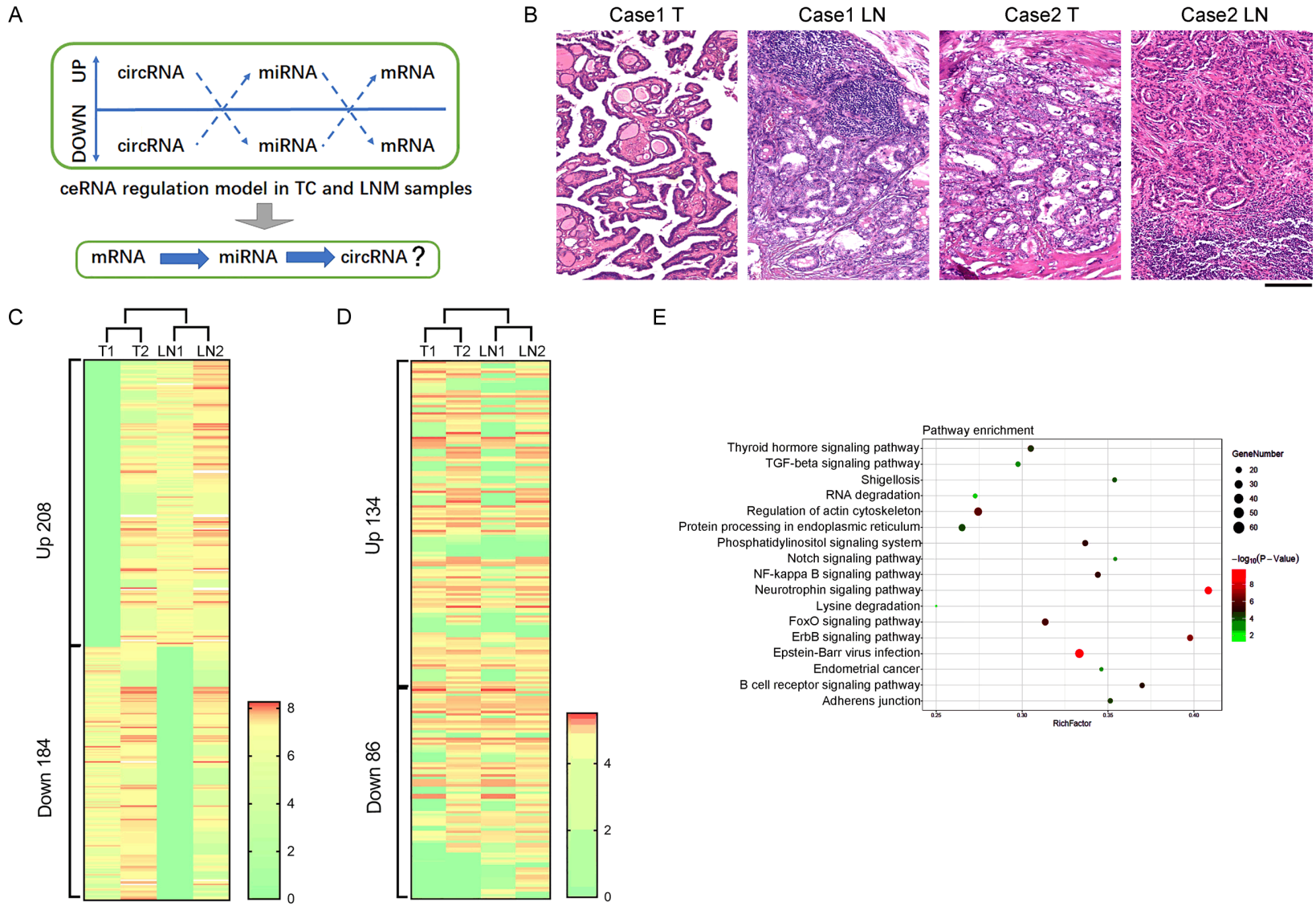
A
UP
DOWN
circRNA
miRNA
mRNA
circRNA
miRNA
mRNA
ceRNA regulation model in TC and LNM samples
mRNA
miRNA
circRNA ?
B
Case1 T
Case1 LN
Case2 T
Case2 LN
C
T1
T2
LN1
LN2
Up 208
Down 184
8
6
4
2
0
D
T1
T2
LN1
LN2
Up 134
Down 86
4
2
0
E
Pathway enrichment
Thyroid hormore signaling pathway
TGF-beta signaling pathway
Shigellosis
RNA degradation
Regulation of actin cytoskeleton
Protein processing in endoplasmic reticulum
Phosphatidylinositol signaling system
Notch signaling pathway
NF-kappa B signaling pathway
Neurotrophin sigaling pathway
Lysine degradation
FoxO signaling pathway
ErbB signaling pathway
Epstein-Barr virus infection
Endometrial cancer
B cell receptor signaling pathway
Adherens junction
0.25
0.30
0.35
0.40
RichFactor
GeneNumber
20
30
40
50
60
−log10(P−Value)
8
6
4
2

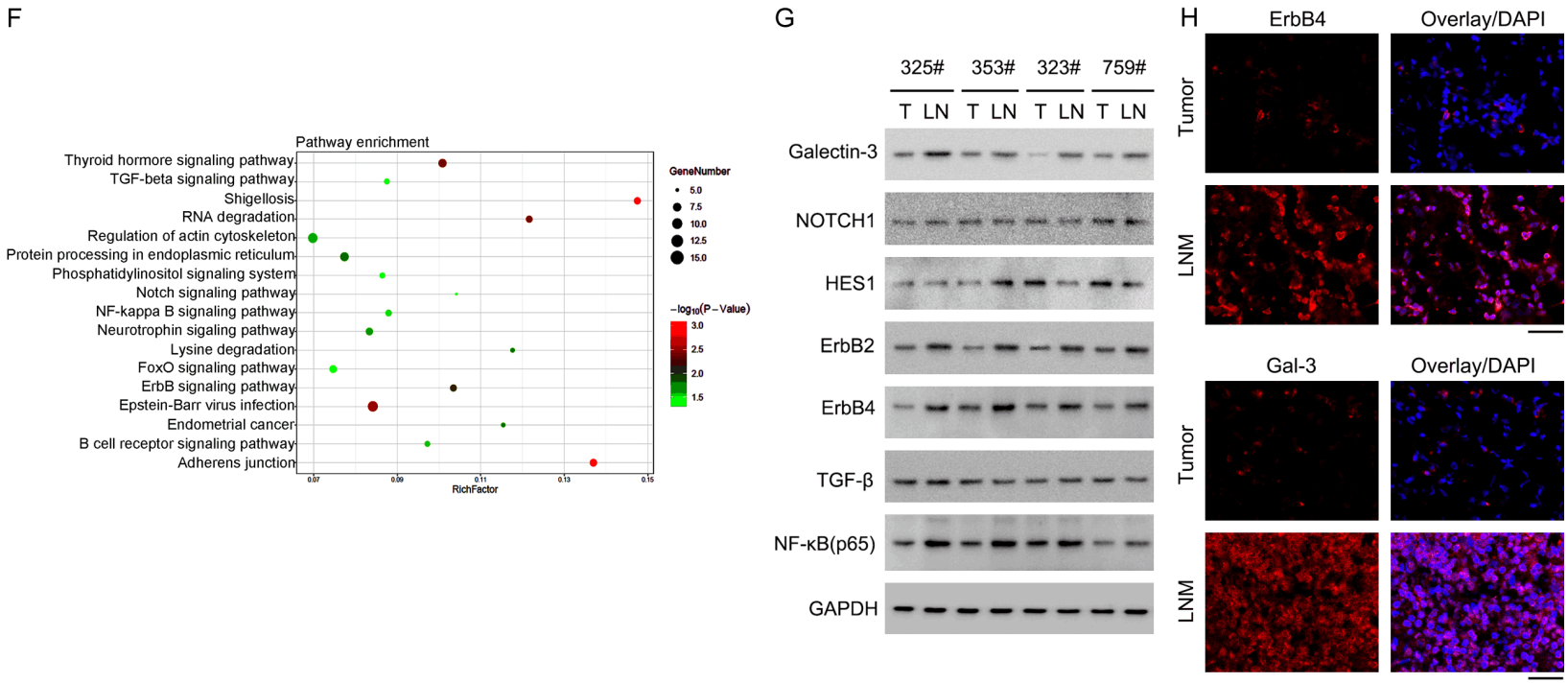


**Figure 2.** Enrichment of miRNA and circRNA sequencing profiles. Flow chart of the circRNA/miRNA/mRNA screen to identify regulators upstream of Gal3 (A). Pathological morphology was validated by HE staining of two paired primary and LNM tumor samples that were prepared for RNA sequencing (B). Unsupervised hierarchical clustering shows distinct miRNA (C) and circRNA (D) expression with green representing decreased expression. Significantly enriched pathways in genes regulated by differentially expressed cancer-related miRNAs (E) and circRNAs (F) were identified by KEGG pathway enrichment analysis. Western blot analysis for ErbB, NOTCH, NF-κB and TGF-β pathways (G). IF staining for Gal3 and ErbB4 in original tumor and Lymph node metastasis tissues (H). bar = 20 μm.

A

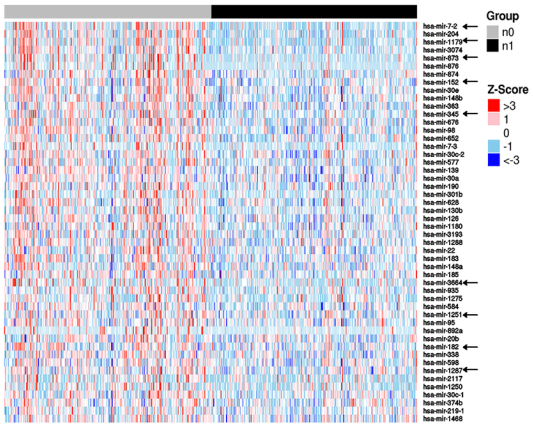


B

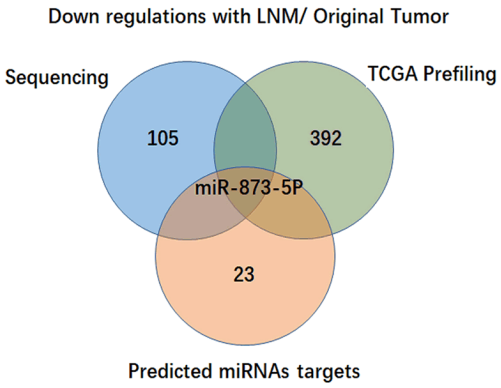


C

```
LGALS3 (Mut)  5' - UAAGAGUCU - TGUACCTATCAU - 3'
LGALS3 (WT)   5' - UAAAGGUUU - CAUGUUCACUGU - 3'
                    ||   |   ||  ||||  |||
hsa-miR-873   3' - UCCUCUGAGUGUUCAAG - GACG - 5'
```

| Speices | Sequence (3'-UTR) | Match number |
|---|---|---|
| Human | UAAAGGUUUCAUGUUCACUGUGAGU | 12 |
| Chimp | UAAAGGUUUCAUGUUCACUGUGAGU | 12 |
| Rhesus | UAAAGGUUUCAUGUUCACUGUGAGU | 12 |
| Jerboa | UAAAGGUUUCAUGUUCACUGUAAGU | 12 |
| Mole-rat | CAAAGGCUUCAGGUUCACUGGGAGU | 12 |
| Bat | UAAAAGUUUCAUGUUCACUGUAAGU | 11 |
| Whale | UAAAAGUUUCAUGUUCACUGUGAGU | 11 |
| Pig | CAAAAGUUUCAUGUUCACUAUGAGU | 10 |
| Elephant | UAAGAGCUUCAUGUUCACUG --AGU | 10 |
| Horse | UAAAGGAUUCAUGUUGACUAGGAGU | 10 |
| Rabbit | UAAAAGCUUUAUGUUCACUACGAGU | 9 |
| Hamster | UAAAGGCUCCGUGUUCAUUCGGAGU | 9 |
| Cat | UAAA --UCUCAUGUUUACUG --ACU | 9 |
| Alpaca | UAAAAGUUUCACGUUCAUUAUGAGU | 8 |

D

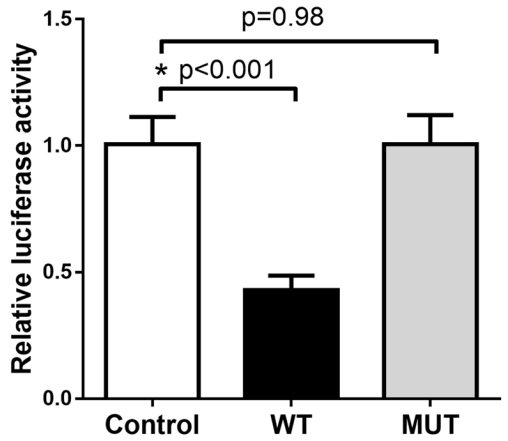


E

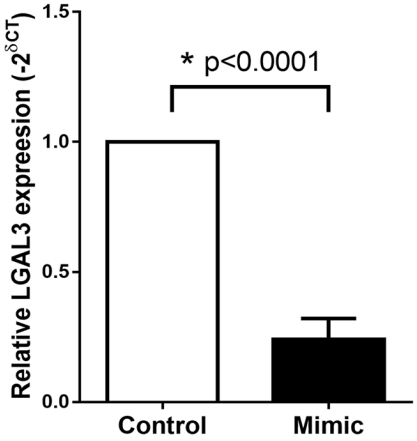


F

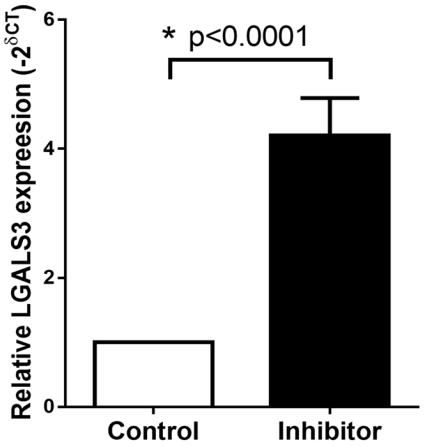

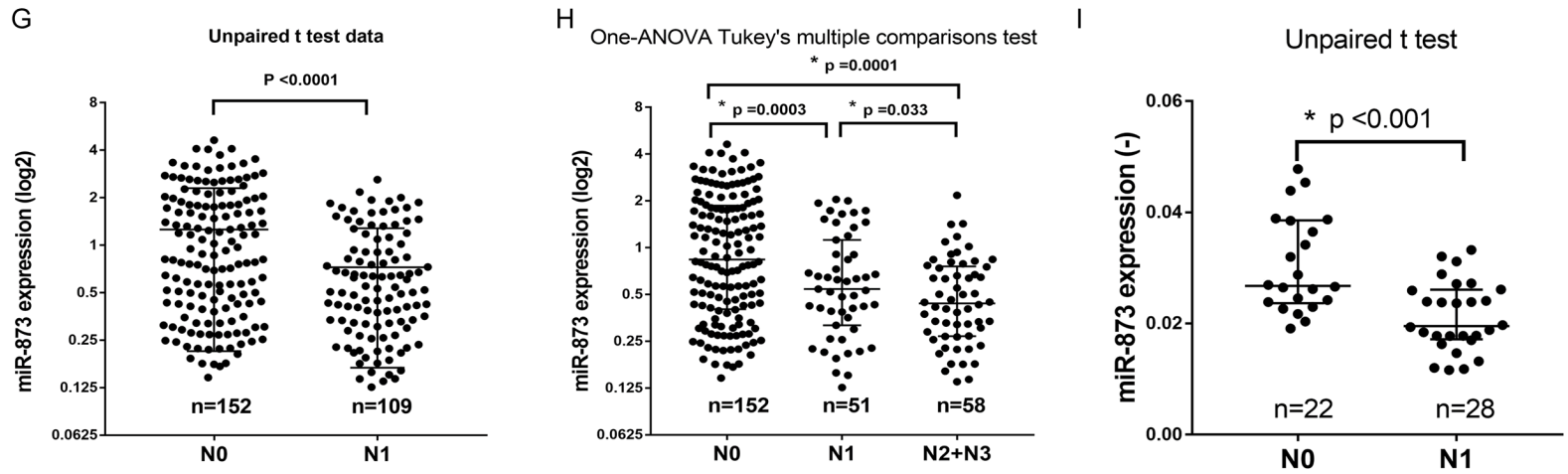


**Figure 3.** miR-873 was identified to act as an upstream regulator of Gal3. Unsupervised hierarchical clustering heat map of miRNA expression fold-change from TCGA data shows the top 50 miRNAs with decreased expression in the LNM group. Nine miRNAs were consistent with our sequencing data, as shown by the black arrow (A). A Venn diagram showing that miR-873 is a potential regulator of Gal3 and is related to LNM in PTC (B). The putative binding site of miR-873-5p on Gal3 is shown, including the wild-type and mutated Gal3 3'-UTR sequences which were used to create the wild-type and mutant luciferase reporter constructs. The similarity between 12 putative complementary binding sites (red letters) of the Gal3 3'-UTRs from different species (C). A luciferase reporter assay demonstrated that miR-873 inhibited the transcription of the wild-type but not the mutant 3'-UTRs of Gal3 (D). The expression of endogenous Gal3 RNA was inhibited in miR-873-mimic-infected HEK293 cells compared to the control, as detected by qRT-PCR and normalized to GAPDH mRNA (E), while it was increased in the miR-873 inhibitor group (F). The RNA level of miR-873 was validated in LNM-positive tumor tissues compared to the negative control by analyzing the TCGA profile. N0: non-LNM; N1: LNM (G). miR-873 was validated again in a different metastatic lymph node group, N0: non-LNM; N1<4; 4<N2<10; N3>10 (H). Relative expression of miR-873 in circulation was detected by qRT-PCR between non-LNM and LNM patients (I). Unpaired t-test and one-way ANOVA multiple comparisons test were performed to obtain *P* values in comparisons of two or more groups. * indicates P<0.05.

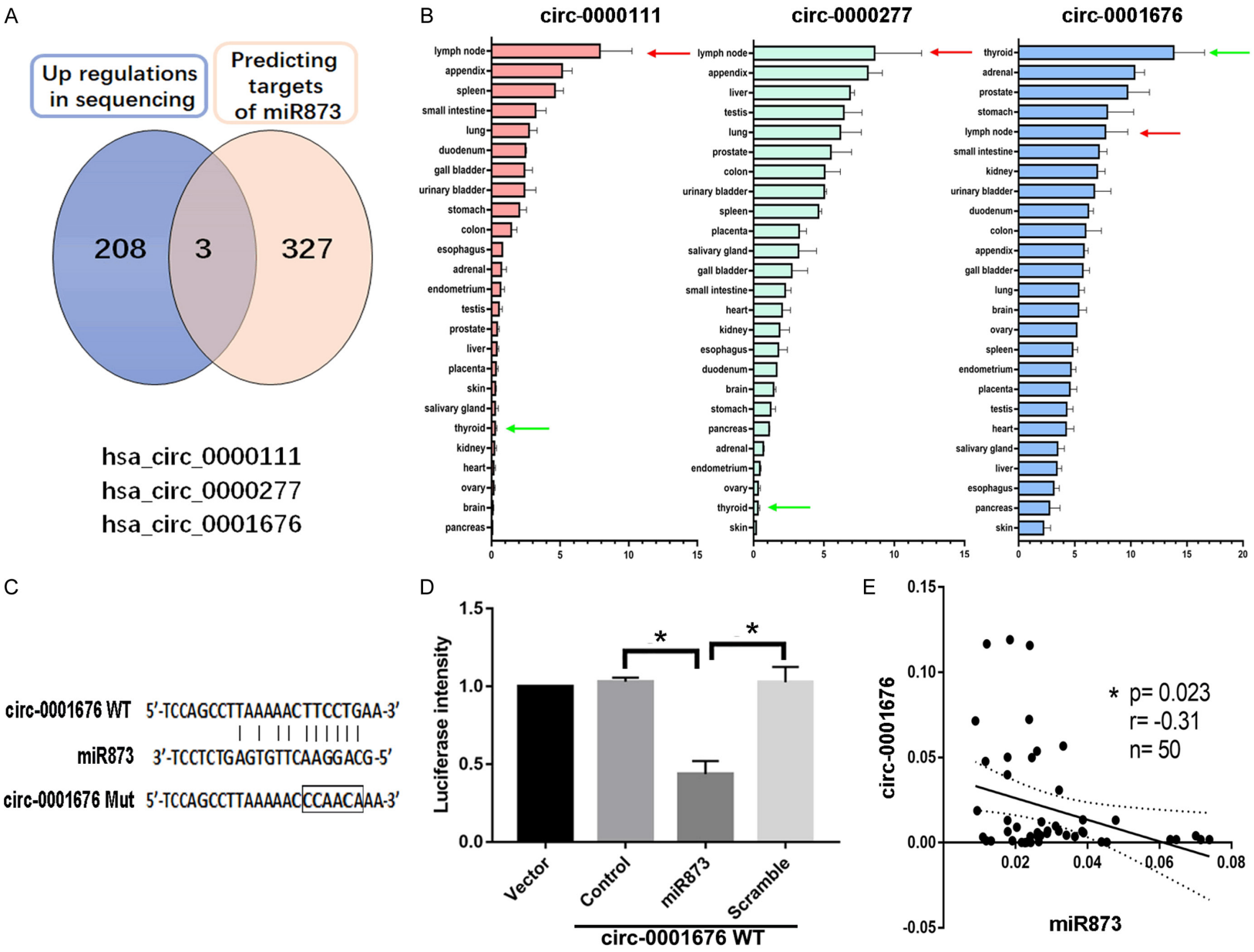
A
Up regulations in sequencing
Predicting targets of miR873
208
3
327
hsa_circ_0000111
hsa_circ_0000277
hsa_circ_0001676
B
circ-0000111
circ-0000277
circ-0001676
C
circ-0001676 WT 5′-TCCAGCCTTAAAAACTTCCTGAA-3′
miR873 3′-TCCTCTGAGTGTTCAAGGACG-5′
circ-0001676 Mut 5′-TCCAGCCTTAAAAACCCAACAAA-3′
D
Luciferase intensity
Vector
Control
miR873
Scramble
circ-0001676 WT
E
circ-0001676
miR873
* p= 0.023
r= -0.31
n= 50

**Figure 4.** Hsa-circRNA-UMAD1 acts as a miRNA sponge to directly target miR-873. Venn diagram identified circRNA-UMAD1 as a candidate sponge for miR-873 through prediction by a circRNA website tool and circRNA sequencing data (A). Three circRNAs were expressed in normal tissues from HPA-RNA sequencing (B). The sequence alignment of the human circRNA sequence and miR-873 is shown. The mutated sequence in the corresponding binding sites of circRNA UMAD1 that was used to generate the firefly luciferase reporter constructs is shown underneath the miR-873 set (C). A luciferase reporter assay was performed to detect the activity of circRNA UMAD1 in HEK293 cells cotransfected with miR-873 or scramble control and circRNA UMAD1 or vector (D). The correlation between the expression of circRNA UMAD1 and miR-873 was evaluated by Person's correlation test in 50 samples (r = -0.31, P = 0.023) (E).

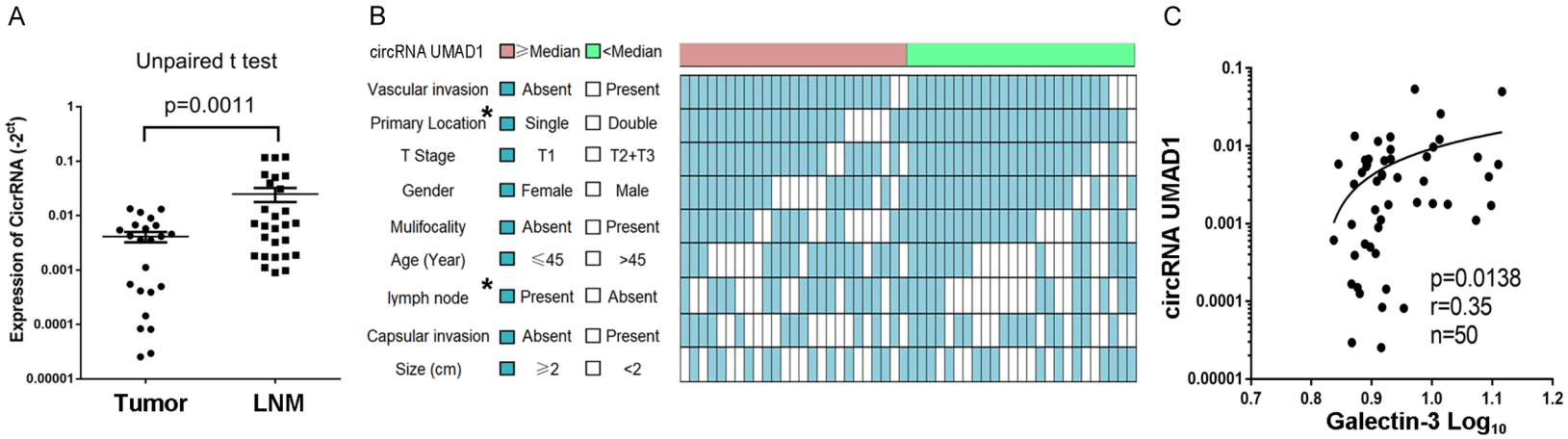


**Figure 5.** CircRNA UMAD1 is associated with LNM and Gal3 expression. Expression of hsa-circ-UMAD1 quantified by at least three independent qRT-PCR experiments in the cohort comparing non-LNM tumors (absent, n = 23) and LNM tumors (present, n = 27). Unpaired t-tests were performed to identify significant differences. The relative expression level of circRNA UMAD1 was normalized to the level of β-actin (A). CircRNA UMAD1 expression was significantly related to LNM and primary side location based on univariant analysis of 50 PTC patients, which is described in **Table 1** (B). The correlation between the expression of circRNA UMAD1 and Gal3 was evaluated by Person's correlation test (r = 0.35, P = 0.00138) (C). All data are expressed as the median ± range with three independent experiments.

**Table 2.** Relationship between circRNA UMAD1 expression and pathological features in PTC patients with or without LNM

| Variable | Case no. | circ expression[1] (RQ: $2^{-\Delta Ct}$) | | $P^2$ | circ expression[1] (ΔCt) | $P^3$ |
|---|---|---|---|---|---|---|
| | | Median | Range | | Mean ± SEM | |
| Gender | | | | 0.4894 | | 0.9755 |
| Male | 12 | 0.06594 | 0.0008924-0.1191 | | 0.01513±0.009511 | |
| Female | 38 | 0.004059 | 0.00002531-0.1166 | | 0.01543±0.004626 | |
| Age (Year) | | | | 0.9027 | | 0.7625 |
| ≤45 | 29 | 0.005759 | 0.00002927-0.1191 | | 0.01580±0.005646 | |
| >45 | 21 | 0.003521 | 0.00002531-0.1166 | | 0.01476±0.006197 | |
| Size (cm) | | | | 0.5414 | | 0.0757 |
| <2 | 24 | 0.004412 | 0.00002927-0.1191 | | 0.01666±0.006479 | |
| ≥2 | 26 | 0.003521 | 0.00002531-0.1158 | | 0.01196±0.004329 | |
| Side location | | | | 0.0229* | | 0.0418* |
| Single (Left or Right) | 44 | 0.004059 | 0.00002531-0.1191 | | 0.01192±0.003844 | |
| Double | 6 | 0.03045 | 0.003521-0.1158 | | 0.04059±0.01801 | |
| Capsular invasion | | | | 0.0508 | | <0.0001* |
| Absent | 26 | 0.003369 | 0.00002927-0.05336 | | 0.007625±0.002654 | |
| Present | 24 | 0.005922 | 0.00002531-0.1191 | | 0.02374±0.007872 | |
| Vascular invasion | | | | 0.3858 | | 0.0011* |
| Absent | 45 | 0.004550 | 0.00002531-0.1191 | | 0.01657±0.004567 | |
| Present | 5 | 0.003521 | 0.00008110-0.009685 | | 0.004460±0.001750 | |
| Lymph node metastasis | | | | 0.0101* | | <0.0001* |
| Absent | 23 | 0.003521 | 0.00002531-0.01332 | | 0.004117±0.0008956 | |
| Present | 27 | 0.006754 | 0.0008924-0.1191 | | 0.02494±0.007184 | |
| T stage | | | | 0.5033 | | 0.0185* |
| T1 | 42 | 0.004770 | 0.00002531-0.1191 | | 0.01659±0.004849 | |
| T2+T3 | 8 | 0.004412 | 0.001106-0.03983 | | 0.008926±0.004516 | |
| Multifocality | | | | 0.0926 | | 0.0041* |
| Absent | 34 | 0.003825 | 0.00002531-0.1166 | | 0.01058±0.003755 | |
| Present | 16 | 0.005990 | 0.0004985-0.1191 | | 0.02552±0.009953 | |

[1]Quantified by qRT-PCR. Cric UMAD1 was normalized to U6. [2]Mann-Whitney U test for the comparison between two groups or Kruskal-Walis test for more groups. [3]Unpaired Student's t-test for the comparison between two groups. *$P$<0.05.

expression of hsa-circ-UMAD1 was higher in the lymph node metastasis tumor than in the primary tumor site. Fifty patients were further analyzed by RT-PCR to determine the correlation between the clinicopathological characteristics and the levels of hsa-circ-UMAD1 (**Figure 5B**). No significant difference was observed between hsa-circ-UMAD1 expression levels based on gender, age, tumor size and vascular invasion. However, the expression of hsa-circ-UMAD1 in the LNM samples was significantly higher than that in primary samples without local tumor invasion (**Table 2**). In addition, hsa-circ-UMAD1 and Gal3 expression levels were significantly correlated with a high R value (0.35, P<0.0138) (**Figure 5C**). Thus, hsa-circ-UMAD1 is a candidate biomarker for predicting the potential risk of LNM in PTC.

*ROC curve analysis of circRNA-UMAD1 and Gal3*

To assess whether the identified circulating circRNA-UMAD1 and Gal3 can serve as potential diagnostic biomarkers for LNM in PTC, ROC curves were generated for qRT-PCR-validated samples. Separating circRNA-UMAD1 and Gal3 in the ROC analysis resulted in unsatisfactory specificity and sensitivity. The areas under the ROC curve (AUC) were 0.8407 for Gal3 and 0.7531 for the circRNA (**Figure 6A**, **6B**). A sensitivity of 59.26% and a specificity of 96.67% were observed in the highest likelihood ratio in

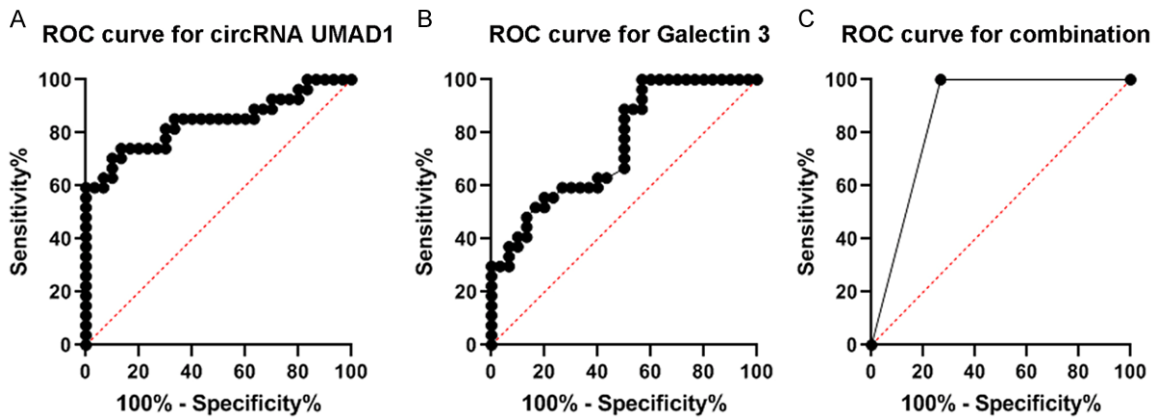


**Figure 6.** ROC curves for individual biomarkers circRNA UMAD1 and Gal3 or combination. ROC curve analysis of circRNA UMAD1 calculates the best cutoff point to discriminate between the LNM and primary tumor groups. The area under the curve (AUC) (SE) = 0.718 (0.072); 95% confidence interval was 0.576 to 0.86; P = 0.0084 (A). ROC curve analysis of Gal3 between these two groups. AUC (SE) = 0.825 (0.061); 95% confidence interval was 0.704 to 0.945; P<0.001 (B). ROC curve analysis of circRNA UMAD1 combined with Gal3 for distinguishing patients in the LNM *vs.* primary tumor groups. AUC (SE) = 0.87 (0.051); 95% confidence interval was 0.766 to 0.97; P<0.001 (C). Likelihood ratio = 3.75. P<0.01, ROC, receiver operating characteristic; SE, standard error.

the Gal3 group. Furthermore, 18.18% sensitivity and 97.83% specificity were observed in the highest likelihood ratio in the circRNA group. Although high specificity was recorded for each target, both sensitivities were still unsatisfactory. Combining the results of the two groups together resulted in 74.07% sensitivity and 100% specificity in predicting the LNM of PTC patients (**Figure 6C**). These results indicate that the combination of circRNA-UMAD1 and Gal3 expression is a sensitive novel biomarker for predicting LNM in PTC patients.

## Discussion

As a tool for prediction of clinicopathological characteristics of PTC, Gal3 is often used for differentiating the malignant tumor [32]. However, the sensitivity of the test is not always satisfactory, especially for testing in the circulation. Since Gal3 is not one of the top genes with the highest expression in LNM samples, we need an additional biomarker to increase the predictive accuracy for diagnosis and balance the specificity and sensitivity with high levels. Form RNA sequencing and bioinformatics analyses in this study, a number of interesting targets were identified that are highly relevant to Gal3 in clinical properties and pathological characteristics. For Gal3 to be a useful biomarker for diagnosing PTC, the diagnostic accuracy of Gal3 in the discrimination of thyroid carcinoma should be over 65% [32]. Compared with the 70.6% sensitivity and 96.8% specificity reported recently [33], 59.26% sensitivity and 96.67% specificity are not good enough to accurately detect minor LNM. Thus, finding an additional biomarker is necessary for widespread use of Gal3 in liquid biopsy, upon which not enough biological tissues for LNM have been confirmed.

Several miRNAs were found to have lower expression in LNM samples in PTC in screens performed by miRNA sequencing and miRNA prediction tools websites. miR-873 was finally selected for use in combination with Gal3 for diagnosing LNM in PTC because in a previous study, miR-873 was part of a signature that identified cancer with lymph node metastases [34]. However, although miR-873 was a direct suppressor of Gal3 in vitro, it is not easily detected in the circulation because of its decreased expression in blood when Gal3 is expressed at high levels in advanced PTC patients or in LNM cases. We attempted to amplify miR-873 by RT-PCR in the peripheral circulation, but we were not successful even after multiple attempts. Notably, analyses of TCGA profiles demonstrated a negative correlation between Gal3 and miR-873 expression in PTC samples. miR-873 is a useful target for the response to Gal3 in tissues but is not suitable for detection in circulation.

Several recent reports have discovered that circRNAs are stable and specific biomarkers by noninvasive detection in plasma [10, 35].

We decided to explore new circRNAs affecting the miR-873-Gal3 axis because circRNAs are closed continuous loops of RNA with miRNA binding sites [10] and can act as sponges of miRNAs to regulate miRNA functions [12]. For this purpose, a circRNA-miR-873-Gal3 interaction was designed and analyzed by the CIRC prediction website. Consistent with the sequencing results, hsa-circ-UMAD1 was identified as a candidate for further screening. We determined that hsa-circ-UMAD1 acts as a miR-873 sponge and inhibits miR-873 expression in vitro. Since circRNAs are relatively stable inside or outside of tumor cells, even exist as ribozymes [36], they are not difficult to extract from fresh blood samples using the correct techniques. CircRNAs in plasma were amplified by RT-PCR and used to analyze the relationship between clinical properties and pathological characteristics. A high level of hsa-circ-UMAD1 expression in the LNM samples was determined to be a novel biomarker for LNM in PTC patients. Fortunately, circRNA-UMAD1 and Gal3 expression were dramatically correlated with a high R value. This evidence suggests that hsa-circ-UMAD1 is a good co-biomarker for the prediction of LNM in PTC. However, the ROC curve of hsa-circ-UMAD1 was a little less than that of Gal3 (AUC: 0.7531 *VS*. 0.8407). After combining the results of the ROC analysis of hsa-circ-UMAD1 and Gal3, 100% specificity was obtained, and the sensitivity was increased from 59.26% to 74.07%. For PTC patients with LNM, double-positive patients for hsa-circ-UMAD1 and Gal3 are at an increased risk for LNM diagnosis.

In this study, we measured circRNA expression in the peripheral circulation of PTC patients with and without LNM by RT-PCR. When circRNA was combined with Gal3 expression in plasma, LNM diagnosis was dramatically improved over single biomarker detection. Further studies are also needed to elucidate the regulatory behavior of the identified circRNA. However, there are still several limitations in our work: the cohort was not large enough, and only 50 samples were included in the independent RT-PCR validation; the prospective cohort study was not designed to specifically test the predictive value of circRNAs and Gal3 detection; and the regulatory mechanism of the identified circRNA, such as ErbB, NF-κB pathways, should be further examined as reported as regulating LNM in PTC via interactions with NF-κB [37] and ErbB pathways [38]. In summary, regardless of the experimental method used, the combination of detecting the levels of both circRNA and Gal3 in the peripheral circulation is an effective co-biomarker for the diagnosis of LNM in patients with PTC. This strategy should be considered as an independent evaluation system for PTC patients with LNM.

## Conclusion

In summary, no matter of what our considered, combination of detecting the levels of circRNA UMAD1 and Gal3 in the peripheral circulation is an effective co-biomarker for the diagnosis in LNM patients with PTC. This strategy should be considered as an independent evaluation system for PTC patients with LNM. PUCH: Peking University Cancer Hospital.

## Acknowledgements

The authors thank the staff at the Department of Cell Biology, Peking University Cancer Hospital and Institute, Beijing 100034, China, for technical support. This study was funded by the National Natural Science Foundation of China (81872025, 81772632), the Beijing Natural Science Foundation (7182030), the Clinical Features Research of Capital (No. Z1511-00004015173), Open Project funded by Key laboratory of Carcinogenesis and Translational Research, Ministry of Education/Beijing (2019 Open Project-03), Natural Science Foundation of Xinjiang Uygur Autonomous Region (2019-D01C264), Science Foundation of Peking University Cancer Hospital 2020-9.

## Disclosure of conflict of interest

None.

## Abbreviations

PTC, papillary thyroid carcinoma; LNM, lymph node metastasis; qRT-PCR, quantitative reverse transcription-polymerase chain reaction; TCGA, The Cancer Genome Atlas; ROC, Receiver operating characteristic curve; AUC, Area under the ROC curve; HPA, Human Protein Atlas; Gal3, Galectin-3; IF, immunofluorescence.

**Address correspondence to:** Dr. Zhiqin Fan, Day Surgery Department, Affiliated Tumor Hospital of Xinjiang Medical University, Urumqi 830011, P. R.

China. E-mail: 491962188@qq.com; Haibo Han, Department of Clinical Laboratory, Key Laboratory of Carcinogenesis and Translational Research (Ministry of Education), Peking University Cancer Hospital and Institute, Beijing 100142, P. R. China. E-mail: haibohan@bjmu.edu.cn

## References

[1] Sapuppo G, Tavarelli M, Russo M, Malandrino P, Belfiore A, Vigneri R and Pellegriti G. Lymph node location is a risk factor for papillary thyroid cancer-related death. J Endocrinol Invest 2018; 41: 1349-1353.

[2] Jeon MJ, Kim YN, Sung TY, Hong SJ, Cho YY, Kim TY, Shong YK, Kim WB, Kim SW, Chung JH, Kim TH and Kim WG. Practical initial risk stratification based on lymph node metastases in pediatric and adolescent differentiated thyroid cancer. Thyroid 2018; 28: 193-200.

[3] Balaji SA, Shanmugam A, Chougule A, Sridharan S, Prabhash K, Arya A, Chaubey A, Hariharan A, Kolekar P, Sen M, Ravichandran A, Katragadda S, Sankaran S, Bhargava S, Kulkarni P, Rao S, Sunkavalli C, Banavali S, Joshi A, Noronha V, Dutt A, Bahadur U, Hariharan R, Veeramachaneni V and Gupta V. Analysis of solid tumor mutation profiles in liquid biopsy. Cancer Med 2018; 7: 5439-5447.

[4] Rolfo C, Mack PC, Scagliotti GV, Baas P, Barlesi F, Bivona TG, Herbst RS, Mok TS, Peled N, Pirker R, Raez LE, Reck M, Riess JW, Sequist LV, Shepherd FA, Sholl LM, Tan DSW, Wakelee HA, Wistuba II, Wynes MW, Carbone DP, Hirsch FR and Gandara DR. Liquid biopsy for advanced non-small cell lung cancer (NSCLC): a statement paper from the IASLC. J Thorac Oncol 2018; 13: 1248-1268.

[5] Rossi ED, Bizzarro T, Martini M, Capodimonti S, Fadda G, Larocca LM and Schmitt F. Morphological parameters able to predict BRAF(V600E) -mutated malignancies on thyroid fine-needle aspiration cytology: our institutional experience. Cancer Cytopathol 2014; 122: 883-891.

[6] Rossi ED, Bizzarro T, Martini M, Capodimonti S, Sarti D, Cenci T, Bilotta M, Fadda G and Larocca LM. The evaluation of miRNAs on thyroid FNAC: the promising role of miR-375 in follicular neoplasms. Endocrine 2016; 54: 723-732.

[7] Perdas E, Stawski R, Nowak D and Zubrzycka M. Potential of liquid biopsy in papillary thyroid carcinoma in context of miRNA, BRAF and p53 mutation. Curr Drug Targets 2018; 19: 1721-1729.

[8] Khatami F and Tavangar SM. Liquid biopsy in thyroid cancer: new insight. Int J Hematol Oncol Stem Cell Res 2018; 12: 235-248.

[9] Fu QF, Pan PT, Zhou L, Liu XL, Guo F, Wang L and Sun H. Clinical significance of preoperative detection of serum p53 antibodies and BRAF(V600E) mutation in patients with papillary thyroid carcinoma. Int J Clin Exp Med 2015; 8: 21327-21334.

[10] Jeck WR and Sharpless NE. Detecting and characterizing circular RNAs. Nat Biotechnol 2014; 32: 453-461.

[11] Rappa G, Puglisi C, Santos MF, Forte S, Memeo L and Lorico A. Extracellular vesicles from thyroid carcinoma: the new frontier of liquid biopsy. Int J Mol Sci 2019; 20: 1114.

[12] Memczak S, Jens M, Elefsinioti A, Torti F, Krueger J, Rybak A, Maier L, Mackowiak SD, Gregersen LH, Munschauer M, Loewer A, Ziebold U, Landthaler M, Kocks C, le Noble F and Rajewsky N. Circular RNAs are a large class of animal RNAs with regulatory potency. Nature 2013; 495: 333-338.

[13] Cai X, Zhao Z, Dong J, Lv Q, Yun B, Liu J, Shen Y, Kang J and Li J. Circular RNA circBACH2 plays a role in papillary thyroid carcinoma by sponging miR-139-5p and regulating LMO4 expression. Cell Death Dis 2019; 10: 184.

[14] Hansen TB, Jensen TI, Clausen BH, Bramsen JB, Finsen B, Damgaard CK and Kjems J. Natural RNA circles function as efficient microRNA sponges. Nature 2013; 495: 384-388.

[15] Pamudurti NR, Bartok O, Jens M, Ashwal-Fluss R, Stottmeister C, Ruhe L, Hanan M, Wyler E, Perez-Hernandez D, Ramberger E, Shenzis S, Samson M, Dittmar G, Landthaler M, Chekulaeva M, Rajewsky N and Kadener S. Translation of CircRNAs. Mol Cell 2017; 66: 9-21, e27.

[16] Schneider T, Hung LH, Schreiner S, Starke S, Eckhof H, Rossbach O, Reich S, Medenbach J and Bindereif A. CircRNA-protein complexes: IMP3 protein component defines subfamily of circRNPs. Sci Rep 2016; 6: 31313.

[17] Lan X, Xu J, Chen C, Zheng C, Wang J, Cao J, Zhu X and Ge M. The landscape of circular RNA expression profiles in papillary thyroid carcinoma based on RNA sequencing. Cell Physiol Biochem 2018; 47: 1122-1132.

[18] Tang W, Huang C, Tang C, Xu J and Wang H. Galectin-3 may serve as a potential marker for diagnosis and prognosis in papillary thyroid carcinoma: a meta-analysis. Onco Targets Ther 2016; 9: 455-460.

[19] Huang L, Wang X, Huang X, Gui H, Li Y, Chen Q, Liu D and Liu L. Diagnostic significance of CK19, galectin-3, CD56, TPO and Ki67 expression and BRAF mutation in papillary thyroid carcinoma. Oncol Lett 2018; 15: 4269-4277.

[20] Zhao W, Ajani JA, Sushovan G, Ochi N, Hwang R, Hafley M, Johnson RL, Bresalier RS, Logsdon CD, Zhang Z and Song S. Galectin-3 mediates tumor cell-stroma interactions by activating pancreatic stellate cells to produce cytokines via integrin signaling. Gastroenterology 2018; 154: 1524-1537, e1526.

[21] Chen C, Duckworth CA, Zhao Q, Pritchard DM, Rhodes JM and Yu LG. Increased circulation of galectin-3 in cancer induces secretion of metastasis-promoting cytokines from blood vascular endothelium. Clin Cancer Res 2013; 19: 1693-1704.
[22] Yilmaz E, Karsidag T, Tatar C and Tuzun S. Serum Galectin-3: diagnostic value for papillary thyroid carcinoma. Ulus Cerrahi Derg 2015; 31: 192-196.
[23] Liu YT, Han XH, Xing PY, Hu XS, Hao XZ, Wang Y, Li JL, Zhang ZS, Yang ZH and Shi YK. Circular RNA profiling identified as a biomarker for predicting the efficacy of Gefitinib therapy for non-small cell lung cancer. J Thorac Dis 2019; 11: 1779-1787.
[24] Vasaikar SV, Straub P, Wang J and Zhang B. LinkedOmics: analyzing multi-omics data within and across 32 cancer types. Nucleic Acids Res 2018; 46: D956-D963.
[25] Wong N and Wang X. miRDB: an online resource for microRNA target prediction and functional annotations. Nucleic Acids Res 2015; 43: D146-152.
[26] Agarwal V, Bell GW, Nam JW and Bartel DP. Predicting effective microRNA target sites in mammalian mRNAs. Elife 2015; 4: e05005.
[27] Georgakilas G, Vlachos IS, Zagganas K, Vergoulis T, Paraskevopoulou MD, Kanellos I, Tsanakas P, Dellis D, Fevgas A, Dalamagas T and Hatzigeorgiou AG. DIANA-miRGen v3.0: accurate characterization of microRNA promoters and their regulators. Nucleic Acids Res 2016; 44: D190-195.
[28] Dudekula DB, Panda AC, Grammatikakis I, De S, Abdelmohsen K and Gorospe M. CircInteractome: a web tool for exploring circular RNAs and their interacting proteins and microRNAs. RNA Biol 2016; 13: 34-42.
[29] Pilli T, Cantara S, Marzocchi C, Cardinale S, Santini C, Cevenini G and Pacini F. Diagnostic value of circulating microRNA-95 and -190 in the differential diagnosis of thyroid nodules: a validation study in 1000 consecutive patients. Thyroid 2017; 27: 1053-1057.
[30] Peng N, Shi L, Zhang Q, Hu Y, Wang N and Ye H. Microarray profiling of circular RNAs in human papillary thyroid carcinoma. PLoS One 2017; 12: e0170287.
[31] Fagerberg L, Hallstrom BM, Oksvold P, Kampf C, Djureinovic D, Odeberg J, Habuka M, Tahmasebpoor S, Danielsson A, Edlund K, Asplund A, Sjostedt E, Lundberg E, Szigyarto CA, Skogs M, Takanen JO, Berling H, Tegel H, Mulder J, Nilsson P, Schwenk JM, Lindskog C, Danielsson F, Mardinoglu A, Sivertsson A, von Feilitzen K, Forsberg M, Zwahlen M, Olsson I, Navani S, Huss M, Nielsen J, Ponten F and Uhlen M. Analysis of the human tissue-specific expression by genome-wide integration of transcriptomics and antibody-based proteomics. Mol Cell Proteomics 2014; 13: 397-406.
[32] Gweon HM, Kim JA, Youk JH, Hong SW, Lim BJ, Yoon SO, Park YM and Son EJ. Can galectin-3 be a useful marker for conventional papillary thyroid microcarcinoma? Diagn Cytopathol 2016; 44: 103-107.
[33] Al-Sharaky DR and Younes SF. Sensitivity and specificity of Galectin-3 and Glypican-3 in follicular-patterned and other thyroid neoplasms. J Clin Diagn Res 2016; 10: EC06-10.
[34] Ozawa T, Kandimalla R, Gao F, Nozawa H, Hata K, Nagata H, Okada S, Izumi D, Baba H, Fleshman J, Wang X, Watanabe T and Goel A. A microRNA signature associated with metastasis of T1 colorectal cancers to lymph nodes. Gastroenterology 2018; 154: 844-848, e847.
[35] Rybak-Wolf A, Stottmeister C, Glazar P, Jens M, Pino N, Giusti S, Hanan M, Behm M, Bartok O, Ashwal-Fluss R, Herzog M, Schreyer L, Papavasileiou P, Ivanov A, Ohman M, Refojo D, Kadener S and Rajewsky N. Circular RNAs in the mammalian brain are highly abundant, conserved, and dynamically expressed. Mol Cell 2015; 58: 870-885.
[36] Zhuang ZG, Zhang JA, Luo HL, Liu GB, Lu YB, Ge NH, Zheng BY, Li RX, Chen C, Wang X, Liu YQ, Liu FH, Zhou Y, Cai XZ, Chen ZW and Xu JF. The circular RNA of peripheral blood mononuclear cells: Hsa_circ_0005836 as a new diagnostic biomarker and therapeutic target of active pulmonary tuberculosis. Mol Immunol 2017; 90: 264-272.
[37] Le F, Zhang JY, Liu W, Huang XM and Luo WZ. The levels of NF-kappaB p50 and NF-kappaB p65 play a role in thyroid carcinoma malignancy in vivo. J Int Med Res 2018; 46: 4092-4099.
[38] Ab Mutalib NS, Othman SN, Mohamad Yusof A, Abdullah Suhaimi SN, Muhammad R and Jamal R. Integrated microRNA, gene expression and transcription factors signature in papillary thyroid cancer with lymph node metastasis. PeerJ 2016; 4: e2119.